Coordination Polymer Particles (CPPs) for Nanomedicine

F. Novio,[1] J. Simmchen,[1] N. Vazquez,[2] L. Amorín,[2] and D. Ruiz-Molina[1]*

[1]Centro de Investigación en Nanociencia y Nanotecnología (CSIC). Campus UAB, 08193 Bellaterra (Spain). Telf.: (+34)93-5814777; Fax: (+34) 93-5813717. E-mail: druiz@cin2.es

[2] Chemistry Department, Universitat Autònoma de Barcelona 08193 Barcelona Spain

Abstracts.

Nanoscale coordination polymers particles (CCPs) have demonstrated excellent and promising expectations for their application in medicine. This review outlines the most recent advances for their synthesis and their notable suitability to be used in nanomedicine as smart drug delivery systems, bioimaging probes or a combination of both. The potential multifunctional character of these nanosystems opens new perspectives in chemistry, pharmaceutical and medical sciences with their application in diagnosis and therapy fields.

1. INTRODUCTION

Polymers have a broad impact in our society for many years due to their applications in several diverse fields such as energy, healthcare or security among many others. Moreover, are consolidating new emerging technological advances into this new century by facing new synthetic and functional approaches. One of such challenges is the opening of new applications derived from the incorporation of metals into polymer systems through the use of coordination chemistry. Coordination polymers (CPs), exhibit some intrinsic advantages associated to the use of metal ions. First, metal-ligand bonds present directional interactions that can be used to systematically control and tune the shape and dimensionality of the polymers opening new avenues for the design of tailored morphologies, from solid platforms to solutions or colloidal particles. And second, they exhibit functional properties associated to the limitless choice of metallic elements they can contain, such as magnetic, electronic, optical and catalytic properties

[1-3]. Moreover, different metal elements also find ubiquitous functions in natural biological systems such as oxygen transport, gene activation and peptidase catalysis [4].

Miniaturization of CPs to the nanometer length scale is a unique opportunity to develop a new class of highly tailorable functional materials that combine the rich diversity of CPs with the evident advantages of nanomaterials. Specifically, medical applications represent a new technological area where nanoscale coordination polymers are expected to have a broad impact. Possible applications will range from the fine-tuning for controlled release of therapeutic agents or imaging applications [5]. Though, challenges remain in the design of particles to be uniform and below several hundred nanometers owing to their size mismatch with nano-/microscale proteins, cells, and tissues [6]. Moreover, nanosized systems can be successfully applied exploiting the EPR (enhanced permeability and retention effect) as a means of passively targeting cancer tissue [7]. Another stringent requirement that such structures must fulfill is their biological compatibility, including stability in physiological environment and at high concentrations of competing ligands. Only in this way the sustained release of imaging or therapeutic cargoes can be achieved upon their delivery to the intended tissues. If successful, coordination therapeutic formulations will offer numerous advantages including enhanced drug accumulation, reductions in systemic toxicity, and the ability to be surface-functionalized with targeting moieties or molecules with additional properties such as fluorescence [8-12]. One of the coordination polymer families most widely used with this aim is that of metal-organic frameworks (MOFs). MOFs allow control over the release cargo by modifying tunable pores with exceptionally high surface areas and therefore loading capacities. The presence of crystalline frameworks also makes easier the analysis of the host-guest interactions and systematic encapsulation/release studies of model drugs combined to modeling techniques. A number of comprehensive highlights summarizing the progress of MOFs for medical applications are available [13] including the excellent review by Horcajada et al. that nicely summarizes the biocompatibility of MOFs and their ability to encapsulate drugs and/or imaging probes [14].

Another family that has attracted especial attention over the last few years is that of spherical coordination polymer particles (CPPs). Preparation of nanoscale CPPs through various techniques (solvothermal reactions, reverse emulsion techniques or fast precipitation) typically involves a very fast precipitation process far from the

crystallization equilibrium resulting in amorphous structures. First reported in 2005 [15,16], the number of publications involving CPPs is exponentially increasing. Examples of fluorescent metal–organic spheres that show selective cation-exchange [17] and hydrogen-storage properties, [18] as well as other examples with an interesting valence tautomeric behavior [19] have been reported. In this review some of the most important achievements concerning encapsulation, drug delivery and bioimaging that have been made in this field to date are summarized.

2. ENCAPSULATION

Encapsulation not only protects the drug from degradation before reaching cancer cells but also protects the non-cancerous cells from the effects of the drug. Moreover peptides, antibodies, or aptamers can be attached to the particle surface for active targeting of cancer tissue [20]. Even though CPPs are not open-framework structures itself as MOFs, some of us recently showed that their tunable matrix composition allows for the encapsulation of different functional guest molecules. The encapsulation process takes place along the self-assembly process of the particle formation and is tuned by the nature of bridging ligands [21]. Following this methodology, the wide-ranging encapsulation capability of such spheres is demonstrated for several types of functional species. For instance, magnetic iron oxide particles (10 nm diameter) are encapsulated within Zn(bix) spheres (with an average diameter of 600 nm). Magnetic measurements performed on the encapsulated spheres exhibit characteristic hysteresis loop with a coercive field of 137 Oe and 20 Oe at 10 K and at room temperature, respectively. The encapsulation of luminescent quantum dots (QDs) and two organic dyes, fluorescein and rhodamine B was also shown to take place. Interestingly, the resulting coordination spheres combine the intrinsic fluorescence properties of the coordination matrix with those characteristics of the encapsulated species. Therefore, QDs/fluorescein/Zn(bix) spheres are fluorescent in the blue, green, and red regions of the spectrum. This allows the multiencapsulation of luminescent species into coordination particles to be envisaged as a potential route towards the development of tunable broadband light sources for imaging applications.

Micro- and nanoscale amorphous coordination polymer particles 300 ± 23 nm in diameter can also be used for encapsulating drugs such as doxorubicin (DOX), SN-38,

camptothecin (CPT) and daunomycin (DAU) with efficiencies up to 21% [22]. The drug release process was afterwards investigated on a colloidal phosphate buffered saline solution (PBS) at 37 ºC and pH = 7.4. Zn(bix) spheres showed a fast release of ~ 80% at 8 hours, followed by an additional release of ~ 15% over the next 2 days, as confirmed by fluorescence spectroscopy. Similar to other encapsulating systems [23-26], the fast release was attributed to both desorption and diffusion of drug as well as to the gradual erosion of Zn(bix) spheres in PBS. In vitro cytotoxicity assays were also done on HL60 (Human promyelocytic leukemia cells) cell line with 24 h and 48 h of incubation. Treatment of HL60 with DOX/Zn(bix) spheres notably reduces the cell-viability down to 25% at 10 mM, whereas the Zn(bix) spheres gives a cell-viability close to 80% (no effect was detected below such concentration). Overall, DOX/Zn(bix) spheres gave a half maximal inhibitory concentration (IC_{50}) of 5.2 mM and 4.5 mM after 24 h and 48 h of incubation, respectively, whereas the non-loaded Zn(bix) spheres had respective IC_{50} values of only 62.5 mM and 99.9 mM. These results suggest that the DOX released from the DOX/Zn(bix) spheres can induce the cell death in cancer cells similar to those treated with non-encapsulated DOX.

-Insert Figure 1 here-

Alternatively, Mao et al. have made use of one-pot encapsulation processes for the formation of CPPs with good bioelectrochemical catalytic activity toward glucose oxidation [27]. The synthesis of such "all-in-one" nanoscale CPPs was based on the use of active nicotinamida adenín dinucleótido (NAD^+). NAD^+acts as a bidendate ligand that coordinates with Tb(III) through the N atoms of the imidazole ring and the phosphate groups. The formed Tb–NAD^+ nanoparticles with diameters ranging from 50 to 100 nm where used to the one-pot co-encapsulation of different functional guest molecules, including metilene green (MG) electrocatalyst and glucose dehydrogenase (GDH) biorecognition units. Their biosensing activity was afterwards studied by dip-coating onto a glassy carbon (GC) electrode. The nanoparticles showed an excellent biosensing response for glucose in phosphate buffer (0.10mM, pH 7.0) with a linear range from 0.25 to 8 mM. This, together with the high stability of the CCPs in water, validate this strategy for biosensing into a physically readable electronic signal. Their use could largely facilitate rapid and on spot measurements in various areas, including social safety guarantee, quality control, clinical diagnostics or environmental monitoring.

3. ACTIVE FRAMEWORKS

An alternative method for releasing high amounts of drugs and/or bioimaging applications consists in the direct incorporation of active species as CPPs building blocks, instead of their encapsulation. The main advantage of this approach is that payloads are expected to be considerably higher though may require more intriguing steps and/or protection (vide infra). This can be done following two different approaches:, I) use of biologically active metal ions (Ag, Zn, Ca, Mn, Gd, Fe, ...) as connecting building blocks and II) use of organic drugs acting as bridging ligands.

3.1 Active metal ions. Wang et al. have shown that Cu-based spherical CPPs made out from 3,5-bis(pyridin-3-ylmethylamino)benzoic acid show stronger activities than the corresponding Zn-based CPPs toward breast (MCF-7) cancers [28]. For this colorimetric assays measuring the cellular activity (MTT tests) were used. Zn-based CPPs were cytocompatible even after 48 h of treatment with cell viabilities well above 72-83% at a concentration of 100 μg/mL. On the contrary, Cu-based CPPs lead to a dose-dependent cytotoxicity in the range of 5−100 μg/mL. IC_{50} values of Cu-based CPPs obtained after 24 and 48 h of treatment were 19.755 ± 1.217 and 4.671 ± 0.199 μg/mL, respectively, slightly higher than those of other Cu-based polymers [29]. This fact has been tentatively attributed to the interaction of CPPs with the cell body or the disassociation of copper ions from CPP and the diverse coordination modes of the copper center [30]. Moreover, these CPPs exhibit certain selectivity against different tumors. In vitro antitumor activities of freshly prepared CPPs show that both Cu- and Zn-based compounds exhibit potent cytotoxicities against the two cancer cell lines HeLa and NCI-H446. Therein, the IC_{50} values of Cu-based compound against HeLa and NCI-H446 after 72 h of treatment are 17.461 ± 4.943 and 30.721 ± 1.257 μg/mL, respectively. The as-synthesized CPPs exhibited good antibacterial and photoluminescence properties, which make them to be promising candidates for potential applications in medical field.

Pt-based CPPs can be as well excellent active systems given that Pt-based drugs are still used as the frontline treatment for a number of cancers [31-34]. With this aim, Li et al. were first to report the obtaining of CPPs from Tb(III) ions that act as metallic nodes and (diamminedichlorodisuccinato) Pt(IV) complexes as binding ligands, upon precipitation from an aqueous solution by the addition of a poor solvent [35]. The as-

synthesized CPPs were structurally amorphous and exhibited a spherical morphology with average diameters of 58.3±11.3 nm measured by DLS in ethanol. Unfortunately, while the nanoparticles are readily dispersible in most organic solvents, nanoparticle formation was reversible if excess water is added in the reaction mixture. To circumvent this problem, the nanoparticles were encapsulated in shells of amorphous silica which stabilized them and allowed to efficiently control the release of the Pt species by varying the silica shell thickness. This modification allowed to increase the half-lives of the nanoparticles from $t_{1/2}$ of ~1 h to several hours. This represents time enough to allow them to keep in the blood stream, circulate throughout the body and accumulate in tumor tissue. Unfortunately, in vitro cytotoxicity on the angiogenic human colon carcinoma cell line HT-29 showed no appreciable cell death even at 72h of incubation. This fact was attributed to the difficulty of platinum species released from the nanoparticles to enter the cell effectively. To enhance their cellular uptake, silyl-derived c(RGDfK) was grafted onto their surface. This small cyclic peptide sequence exhibits high binding affinity for the $\alpha_v\beta_3$ integrin upregulated in many angiogenic cancers. The resulting nanoparticles gave IC_{50} values of 9.7 and 11.9 μM depending on the silica thickness, suggesting that the targeted nanoparticles are now sufficiently internalized presumably via receptor-mediated endocytosis. Once inside the cells, the platinum species released from the silica-coated nanoparticles could then be reduced to the active Pt(II) species by intracelular reductants that are present in high concentrations.

-Insert Figure 2 here-

More recently, Shen et al. have also reported backbone-type platinum (IV)-coordinated polymer conjugates prepared by using platinum (IV) prodrugs diamminedichlorodihydroxyplatinum (DHP) or its dicarboxyl derivative diamminedichlorodisuccinatoplatinum (DSP) as co-monomers [36]. The polymers had good water-solubility, and high and fixed platinum loading contents. Cyclic voltammogram studies showed that Pt (IV) in the polymers was much easier reduced to Pt (II) than that in the monomer, particularly at the acidic pH. Thus, these polymers were intracellular reduction-responsive backbone-type polymer conjugates that could be degraded and release Pt (II) species. These conjugates not only had high and fixed platinum contents (between 25-30%), but also showed increased cytotoxicity compared with corresponding Pt (IV) monomer toward various tumor cell lines. In vivo, compared to the monomer DSP, the conjugates had slower blood clearance, better tumor

accumulation and lower platinum levels in most normal organs than the monomer DSP. Therefore, these platinum (IV)-coordinated polymers represent a new class of backbone-type Pt(IV) drug conjugates useful for cancer chemotherapy with notable advantages concerning the monomeric species. The use of Pt(II) in CPPs is more complicated because of its square-planar coordination sphere that could give different structures due to the presence of Pt-Pt interactions [37].

3.2 Drugs as bridging ligands. Very recently, Che et al. described the synthesis of four physiologically unstable anticancer drug-metal nanoparticles covered with pH-responsive coordination polymers [38]. In a first step CPPs were obtained by combination of antifolate therapeutic agent methotrexate (MTX) and the human glyoxalase I inhibitor S-(N-p-chlorophenyl-N-hydroxycarbamoyl)glutathione (CHG) with nontoxic biocompatible and metabolizable metal ions such as zinc or iron. Unfortunately the resulting nanoparticles were unstable in physiological conditions. To circumvent this fact, a Zn-Bix based shell (drug-metal@BIX-Zn) was added generating more stable nanoparticles of average size of 150 nm. Interestingly, the external shell can be disrupted by reduction of external pH, exposing the internal drug-metal cores to the medium with the subsequent release of the drug (vide infra).

-Insert Figure 3 here-

MTX building blocks have also been recently incorporated in CPPs with either Zn^{2+}, Zr^{4+}, or Gd^{3+} ions as the metal-connecting with exceptionally high drug loadings (up to 79.1 wt%) [39]. Zn-based CPPs with average diameters between 40 and 100 nm show a considerable tendency to aggregate, being difficult to stabilize by additional coating (either silica or a lipid bilayer) due to their chemical instability along the process. More robust were Zr-CPPs due to the stronger strength of the Zr-carboxylate bond. In this case, spherical particles with average diameters of 70-180 nm and a zeta potential (1 mM aq. KCl) of –27.2 mV were obtained. This negative zeta potential, along with their stability in water, allows for the coating of these particles with a cationic lipid though failed providing any significant stabilization over the as-synthesized particles in phosphate buffered saline (PBS) or simulated body fluid (SBF). The half-life ($t_{1/2}$) for both coated and bare particles was approximately 2.5 h in PBS and 0.5 h in SBF at 37 ºC and pH 7.4. This fact has been attributed to the strong driving force in forming $Zr_3(PO_4)_4$ in the presence of phosphate ions. For this reason it was necessary to find a

metal less labile than zinc, but with a phosphate K_{sp} much greater than that of $Zr_3(PO_4)_4$. With this aim, gadolinium was the metal of choice. Gd-MTX spherical nanoparticles ranging from 70 to 200 nm and a zeta potential of -10.0 mV were obtained. Moreover their $t_{1/2}$ was increased from 2 h in 8 mM PBS at 37 ºC up to 23 h after encapsulation in a lipid bilayer. Moreover the authors were able to conjugate anisamide (AA), known to target overexpressed receptors in many cancer cell, into the liposomal formulation before lipid coating. Both families of particles (with or without AA) showed enhanced efficacy compared to free MTX in vitro against Jurkat human ALL cells. In addition, lipid-coated nanoparticles were also doped with approximately 10 mol% of a carboxylated $Ru(bpy)_3^{2+}$ derivative that allows the monitoring of MTX uptake by confocal microscopy and thus adecuate this platform to be used for optical imaging.

Nitrogen-containing bisphosphonates (N-BPs) have been also successfully used for the fabrication of CPPs. N-BPs are effective antitumor agents that inhibits matrix metalloproteinase activity and down-regulates integrins [40]. However, their effective anticancer activity has been restricted due to their unfavorable pharmacokinetics, as majority of the injected N-BP dose either binds to the bones or is quickly cleared via renal filtration. To circumvent this limitation, Li et al. have incorporated two N-BPs, pamidronate (Pam) and zoledronate (Zol) directly into crystalline particles using Ca^{2+} ions as the metal-connecting points [41]. The as-synthesized particles in this case are crystalline rod–like structures that can go up to a few micras large and a few hundreds of nanometers width. While stable in water, decompose gradually in 5 mM phosphate-buffered saline (PBS) solution at 37 ºC with a $t_{1/2}$ of 6.3 h (Pam-derivates) and 15.8 h (Zol-derivates). To slow down the dissolution in biologically relevant media, the CPPs were coated with single lipid bilayers (SLBs) containing 1 : 1 (by mol) DOTAP/DOPE (DOTAP = dioleoyl trimethylammonium propane and DOPE = dioleoyl L-a-phosphatidylethanolamine). Success on the coverage of individual particles with SLBs was supported by TEM studies using uranyl acetate stain and confirmed by the release profiles in 5mM PBS at 37 ºC. These last studies showed an increase of $t_{1/2}$ from a few hours up to 120 h and 140 h depending on the nature of the N-BP. In vitro cytotoxicity assays on H460 cells showed that neither the free drug nor the as-synthesized CPPs lead to any appreciable cell death as a result of their inability to enter the cells. On the contrary, lipid coated, with or without functionalized targets, showed significantly higher potency, with IC_{50} values around 4.5 ± 3.4 and 1.0 ± 0.5 mM respectively. As

claimed by the authors, this fact has been attributed to the fusion of the cationic lipid bilayers with cell membranes and s receptor-mediated endocytosis.

-Insert Figure 4 here-

4. STIMULI-RESPONSIVE DELIVERY SYSTEMS

The lability of coordination bonds allows for the fabrication of a new generation of CPPs exhibiting responsive properties that may account for control on the targeted delivery. One of the external stimuli shown to be more active is pH. The formation and cleavage of coordination bonds is sensitive to external pH variations because both metal ions and protons are Lewis acids that compete to combine with the ligand, which is a Lewis base. Moreover, such pH-responsive behavior may result of special value due to the intrinsic pH alterations found in natural and tumoral systems for intra- and extracellular media. In fact, Nature is already taking advantages of this fact. For example, during the process of transferrin recycling in cells [42], iron ions are transferred from the extracellular environment into the cytoplasm by the formation and breakage of coordination bonds in response to a pH change.

Che et al. have exploited this phenomenon to prepare nanoparticles that give rapid and quantitative release of ligands subject to pH regulation [43]. Initially the authors reported four types of drug-based CPPs resulting from the combination of daunorubicin hydrochloride (DNR) and doxorubicin hydrochloride (DOX) with two different metal ions (Cu/Fe). The resulting nanoparticles were monodispersed spheres with diameters in the range of 50–100 nm. The amounts of DNR and DOX released from these nanoparticles suspended in solutions at pH 7.4 were less than 5 and 15% over 24 h, respectively. When the pH of the suspending medium was decreased stepwise from 7.4 to 4.0, it was found that the nanoparticles instantly dissolved due to the cleavage of the coordination bonds except for the DOX-Fe where 77% of the starting nanoparticles are recovered. This fact has been attributed to the weak pH sensitivity of the Fe–ligand coordination bonding strength. To circumvent this situation, an alternative strategy involving the combination with a supramolecular polymer that acts as the host molecule through metal ions is proposed. Then, nanoparticles containing mitoxantrone (MX) coordinated to copper (MX–Cu) were fabricated though unfortunately they did not

release the ligand even in a highly acidic medium due to its strong coordination bonding. To solve this limitation, a new polymer with higher pH sensitivity towards metal coordination such as polyethylene glycol (PEG) was introduced in the reaction mixture. The resulting PEG-Cu-MX spherical nanoparticles (aprox. 50 nm in diameter) exhibited in this way a responsive release at pH below 6 that is influenced by the amount of PEG added. On the contrary, the alizarin red S (AR–Co, AR–Zn) and 1,10-phenanthroline (PTL-Cu) nanoparticles, were highly unstable even in the pH 7.4 solution. To endow the particles with appropriate pH sensitivity through "host-metal" coordination bonds, "host-metal-ligand" architectures were performed by addition of oligochitosan (CTS) on the systems with the aim of strength the linkage. With this modification no ligand release was observed at pH 5–7 mainly because of the excessive strength of the CTS–metal coordination bonds. Such strength is modified and tuned in a successive step simply by introducing as fourth partner the surfactant Pluronic F127 into the CTS–metal–AR/PTL system. As a result, monodispersed nanoparticles were obtained with diameters in the 50–400 nm range. These "double host-metal-drug" systems showed good pH sensitivity for ligand release between pH 7.4 and 4.0 almost in a quantitative manner.

-Insert Figure 5 here-

In a subsequent work, the same group reported an elegant implementation of the previously reported pH-sensitive systems to protect nanoparticles made out of drugs with weak coordination bonding capacities under physiological conditions (such as carboxylates) [38]. CPPs combining antifolate therapeutic agent methotrexate (MTX) and the human glyoxalase I inhibitor S-(N-p-chlorophenyl-N-hydroxycarbamoyl)glutathione (CHG) with nontoxic biocompatible and metabolizable metal ions such as zinc or iron and Calcein-Fe CPPs were obtained by a poor solvent precipitation method. The CPPs are unstable under physiological conditions and precipitate because reaction between phosphate ions and metal ions and fine dissolution of carboxylate agents in physiological solution. To improve such intrinsic stability, a pH-sensitive shell with BIX-Zn coordination bond around the ‘‘drug-metal’’ cores, is growth generating (drug-metal@BIX-Zn) CPPs with average diameters estimated to be between 235 and 180 nm. The breakage of the coordination bond in the shell, triggered by a reduction in external pH, leads to the ablation of shells and the exposure of ‘‘drug-metal’’ CPN cores into the surrounding environment and subsequent release of drug

from the cores. The release amounts of CHG, MTX and Calcein from drug-metal@BIX-Zn nanoparticles suspended in solutions at pH 7.4 are less than 10% over 24 h, indicating that all of the core–shell CPNs are stable for a long time under physiological conditions. As the pH of the suspending medium was gradually adjusted from 7.4 to 4.0, the released amounts of the three drugs in solution were gradually increased. At pH 4.0, 100% of drugs are released, except for Calcein (90%). The total drug content in the core–shell CPPs oscillated between 1.7 and 6.2% in the best of the cases by comparison with the 65-89% range obtained for the drug-metal cores.

5. BIOIMAGING

A number of molecular imaging techniques have been developed for imaging in vitro and in vivo such as positron emission tomography (PET), single photon emision computed tomography (SPECT), ultrasound imaging (USI), magnetic resonance imaging (MRI) or optical imaging (OI). However, the bioimaging technologies using nanoparticles are focused on MRI and OI, mainly based on metal core nanoparticles with magnetic or luminescent properties. On the contrary, the number of systems based on coordination polymers are scarce despite the great potential that they offer because their chemical versatility and facility to tune. Therein we describe some of the most important works including CCPs.

5.1. Magnetic Resonance Imaging (MRI). MRI is one of the most important non-invasive imaging techniques used in clinics based on the nuclear magnetic resonance of the various interacting nuclei, with most imaging applications focusing on proton resonance. These are typically paramagnetic or super-paramagnetic materials, functioning by reducing relaxation times of nearby protons. Previously, the most used contrast agents to enhance the tissue contrast was Gd^{3+} [44]. However, it was found that these systems suffer from drawbacks such as Gd^{3+} ion exchange with endogenous metals (e.g., Zn, Cu) and uptake of complexes in extrabascular space [45] or several cases of nephrogenic system fibrosis (NSF) on patients taking Gd-based contrast agents [46-48], which suggests a need of finding alternatives. Iron oxide nanoparticles have been then extensively studied as contrast agent, especially for imaging reticuloendothelial system (RES) [49-51]. However iron oxide nanoparticles induce hypointensities or interfered with magnetic susceptibility artifacts with the subsequent

inaccurate diagnosis [52]. In this scenario manganese-containing nanoparticles with comparable relaxivities seem to be an attractive alternative to built multifunctional nanoplatforms [53]. Alternatively, Lin et al. have reported the synthesis of Gd-based nanoscale metal-organic frameworks with extraordinarily high MR relaxivities [54]. The toxicity of leached Gd^{3+} ions however precludes clinical applications of these NMOFs. Therefore, taking advantage of the modular nature of coordination polymers through a judicious choice of metal ions and organic linkers these materials can be prepared in a more biocompatible and less toxic manner. With this aim Lin et al. have recently reported the synthesis of nanoscale coordination particles with controllable morphology based in Mn^{2+} that are much less toxic than Gd^{3+} centers [55]. These new nanostructures have been shown to exhibit very high in vivo longitudinal (r1) MR relaxivities by binding to intracellular proteins [56]. Terephthalic acid (BDC) and trimesic acid (BTC) have been used as bridging ligands and the resulting nanostructures coated with a thin silica shell. The coating with silica shell affords stability to the system and facilitate the functionalization with the fluorophore and the surface functionalization with a cell targeting molecule, c(RGDfK) peptide, which enhances their delivery to cancer cells Moreover, such a core-shell nanostructure platform can be used for targeted delivery of other imaging and therapeutic agents.

-Insert Figure 6 here-

5.2.Photoluminiscence for cell imaging. Most nanoparticle-based optical imaging agents are based in quantum dots (QDs) o dye-doped QDs since they are photochemically and metabolically stable, brighter and with a tunable emission spectrum [57-62]. However, this systems also present some problems associated with toxicity, photo oxidation and water solubility [63,64]. An efficient alternative could be the use of quantum dots based on coordination polymers, which have not been reported due to the difficulty in preparing such structures with diameters well below 10 nm. Only recently, Liu et al. have demonstrated a facile approach for rationally constructing quantum dots of coordination polymers from metal ions (Zn^{2+}) and organic molecules (3,4,9,10-perylenetetracarboxylic potassium) [65]. The nanoparticles exhibit an average diameter of 3 ± 0.5 nm that can be controlled to generate a highly uniform distribution by changing the conditions of reaction. Moreover, their optical characterization indicates that the new nanoparticles possess a distinct quantum effect of high photoluminescence in addition to exhibit excellent water-dispersion ability and robust

photostability, which are ideal properties for cellular probes. With this aim, the as-prepared nanoparticles were used as fluorophores to label A498 living cells with photoluminescence evident in the intracellular region. The fluorescence of the labeled cells was maintained at almost the same intensity under 455 nm light irradiation for 3 min. Afterwards, though the intensity decreased slightly with longer irradiation times, the fluorescent intensity was outstandingly stable, maintaining more than 50% of the original intensity, even after irradiation for 20 min. In contrast, the fluorescent signals of cells imaged with traditional fluorescein isothiocyanate (FITC) dye disappeared in only 2 min because of severe photobleaching of the dye. The results indicate that the photoluminescence of the new coordination-based QDs is close to that of inorganic semiconductors QDs and definitively superior when compared to traditional fluorescent dyes. Moreover, the cell viability remained at nearly 100% after 24 h incubation of A498 cells with the same concentration of coordination-based QDs as that used in the cellular imaging experiment, which indicates they possess an excellent biocompatibility.

-Insert Figure 7 here-

Xu et al. have also fabricated novel lanthanide hollow microspheres employing 4,4',4''-benzene-1,3,5-triyl-tri-benzoic acid (H_3BTB) as reactants via a mixed-solvothermal method without using surfactants or templates [66]. SEM and TEM images indicate a large amount of spheres with a size distribution of 260–500 nm in diameter and a hollow structure built from numerous nanoparticles. Results show that multicolor emission ranging from green to red can be realized in these materials by varying the doping concentration of Eu^{3+}. In particular, white-light emission was achieved at an excitation wavelength of 316 nm, which may offer a facile way to obtain white-light emission. As a result of their hollow and porous structure, and excellent photoluminescence properties, they may find extensive applications in bioimaging combined with drug delivery, and their relevant technologies.

Simultaneously, Kimizuka et al. reported a novel approach to synthesize photofunctional nucleotide/lanthanide complexes by inclusion of guest cofactor molecules [67]. A combination of 2'-deoxyadenosine 5'-monophosphate (dAMP) and terbium (Tb^{3+}) in water generates aggregate nanoparticles with average diameter of 30 nm. When the adenine chromophore in the resulting aqueous solution was excited at 260 nm, emission from Tb^{3+} was not observed confirming the absence of energy

transfer from adenine to Tb^{3+}. Though, addition of 3-Hydroxypycolinic acid in the reaction mixture (or even over the preformed nanoparticles) induces the replacement of coordinating water molecules in the coordination sphere of Tb3+ leading to luminescent CPPs. The degree of photoluminescence can be modified in function of cofactor concentration. Thus, the emission increases with the cofactor concentration until a limit of 120μM.

5.3. Combinations. Yang et al. have reported a general method to prepare magneto-phosphorescent nanoscale CPPs (denoted as *f*-CPPs) by combining phosphorescent carboxyl-functionalized Ir^{3+} complexes with magnetic Gd^{3+} ions, providing a promising candidate for phosphorescence and magnetic resonance imaging [68]. These CPPs were uniform hollow spheres with an average diameter of around 60 nm and a wall thickness of about 10 nm. CPPs can also be modified with PVP to improve their water solubility and be used as a bioprobe for phosphorescence and magnetic resonance imaging. The resulting nanosystem, with hydrodynamic diameter about 195 nm is fairly stable in water and PBS buffer at room temperature, which is also essential for them to be used for further biological applications. Moreover, they exhibit intense red phosphorescence, moderate longitudinal relaxivity (r1) and low cytotoxicity. Moreover, inductively coupled plasma atomic emission spectroscopy (ICP-AES) and confocal laser scanning microscopy (CLSM) confirmed f-CPPs@PVP could be taken up by living cells effectively. Therefore, they should be a novel nano-bioprobe for the multimodal imaging of cancer cells.

6. BIOCOORDINATION POLYMER PARTICLES

One of the possible limitations for the use of CPPs in biological systems is the potential harmful that some ligands can exhibit, even though they are coordinated to nontoxic metal ions. For this reason, an experimental approach that appeared recently is the use of biomolecules as ligands to fabricate the nanoparticles named as nanoscale biocoordination polymers (BCPs) . Moreover, this new family of bioparticles may give new insights from a scientific point of view for understanding many biorelated self-assembly processes. Though, and in spite of their interest, biomolecules have multiple possible metal binding sites and the potential to confer chirality and biological activity, increasing the difficulty to construct nanoscale BCPs with hierarchical structures. Most

likely for this reason only a few examples have been reported, remaining the design and construction of nanoparticles with different dimensions, control over chirality and helicity and their chemical functionalization for potential bioapplications as a challenge [69]. For example, through precisely controlling the interaction among metal ions and functional groups, BCPs were used to generate some inorganic oxides and sulfides [70-73]. Nevertheless, as BCPs are constructed using biomolecules as the bridging ligands, the most important applications should be in biological systems.

Two different families of biomolecules can be used with this aim, rigid nucleobases, or flexible biomolecules such as aminoacids or peptides. Among them, aminoacids are the most used ligands for built theses systems because they provide many sites for metal coordination and their chirality influence the dimensionality and structure of the BCPs [74]. First, BCPs made of metal–histidine [75] or metal–glutamate [76] can serve as model systems for studing metal–protein interactions. This approximation not only help us to understand many biorelated processes, such as the cause of heavy metal poisoning, but also make a good foundation for exploitation of new drugs. Second, some BCPs have been directly used in organisms as drug or drug delivery carriers owing to their good biocompatibility and tunable porous structures. For instance, AgI/biomolecule BCPs are good candidates to be used as antimicrobial agents in medicine [77,78].

-Insert Figure 8 here-

7. SUMMARY

Nanoscale CPPs have already shown a great potential for theranostics in spite of being at relative incipient stages of development. Different drug uptake and release routes have been explored. Even though this family of particles do not exhibit an open-framework structure, they have been shown to encapsulate different drugs with yields as high as to 21% with respect to the initial quantity of drug in solution. While the coordination framework does not exhibit any toxicity (whenever the proper choice of metal ions and ligands is done), the released drugs have been shown to have IC_{50} values similar to those of the free drug. Much better encapsulation yields can be obtained by the incorporation of the drugs directly as constitutive units of the coordination network in the form of active ligands or connecting metal ions such as Pt(IV) complexes. Upon

exposure to a given physiological media, the active units are released to the media showing suitable efficiencies. Both experimental approaches can similarly be used for the fabrication of bioimaging probes. Therefore, nanoscale CPPs open an interesting research line in which the versatility and variety of the coordinate polymeric complexes offer an infinity of combinations to develop new materials with ever-improved properties.

However, for this to be achieved there is still a lot of work to do. One of the first issues to be addressed is to understand, and therefore having control, of the mechanisms that control the release of the active principles. Depending on the approach, this could involve gaining control over the kinetics of diffusion, degradation of the nanostructure (which does not necessarily involve chemical degradation) or a combination of both. Delivery through diffusion is modulated mainly by host-guest interactions while that of degradation though nanoparticle-body fluid interactions. In fact, related with this last issue, another challenge to be faced is the synthesis of stable and monodisperse colloidal solutions. Two strategies are to be followed, playing with the nature of the metal ions and ligands (though this approach could be limited by the need to incorporate active drugs) or surface modification. From our understanding, the second approach is expected to create more expectatives not only because its inherent chemical flexibility but also because it will also allow for further surface modification of the nanoparticles with other active units such fluorophores, PEG or even antibodies. We should not forget that most of the particles reported still exhibit dimensions too high for their clinical use, being mostly required to be well below 100 nm.

Finally, even though their effectiveness has been demonstrated in vitro, it will be required pursuing the analysis up to the biodistribution of the material, including the cellular transit, degradation, excretion mechanisms, physiological barrier penetration, chronic toxicity. In vivo studies of the pharmacokinetics and efficiency of the drug-containing nanoCPPs will be the major next steps to evaluate their real performances in medicine. These systems will allow following both detection of the drug-loaded nanoparticles and efficacy of a given therapy, opening challenging perspectives for “theranostics” or the personalized therapy.

ACKNOWLEDGMENT

D. R.–M. wants to thank the Spanish government for economical support through grant MAT2012-38318-C03-02. F. N. and N. V. want to thank the Spanish government for their JdC and FPU grants, respectively. J. S. wants to thanks the CSIC for her JAEDoc grant.

BIBLIOGRAPHY

[1] J. C. Bailar, Prep. Inorg. React. 1 (1964) 1.
[2] E. A. Tomic, J. Appl. Polym. Sci. 9 (1965) 3745.
[3] H. Shindo, T. L. Brown, J. Am. Chem. Soc. 87 (1965) 1904.
[4] X. Wang, R. McHale, Macromol. Rapid Commun. 31 (2010) 331.
[5] Z. Ma, B. Moulton, Coord. Chem. Rev. 255 (2011) 1623.
[6] A. Albanese, P. S. Tang, W. C.W. Chan, Annu. Rev. Biomed. Eng. 14 (2012) 1.
[7] E. Ruiz-Hernández, A. Baeza, M. Vallet-Regí, ACSNano 5 (2011) 1259.
[8] M De, P. S. Ghosh, V. M. Rotello Biology, Adv. Mater. 20 (2008) 4225.
[9] M. Ferrari, Nat. Rev. Cancer 5 (2005) 161.
[10] L. Zhang, F. X. Gu, J. M. Chan, A. Z. Wang, R. S. Langer, O. C. Farokhzad, Clin. Pharmacol. Ther. 83 (2007) 761.
[11] D. Peer, J. M. Karp, S. Hong, O. C. Farokhzad, M. Rimona, R. Langer, Nat. Nanotechnol. 2 (2007) 751.
[12] O.V. Salata J. Nanobiotechnology 2 (2004) 3.
[13] E. A. Flügel, A. Ranft, F. Haase , B. V. Lotsch, J. Mater. Chem. 22 (2012) 10119
[14] P. Horcajada, R. Gref, T. Baati, Ph. K. Allan, G. Maurin, P. Couvreur, G. Ferey, R. E. Morris, Ch. Serre, Chem. Rev. 112 (2012) 1232.
[15] M. Oh, C. A. Mirkin, Nature 438 (2005) 651.
[16] X. Sun, S. Dong, E. Wang, J. Am. Chem. Soc. 127 (2005) 13102.
[17] M. Oh, C. A. Mirkin, Angew. Chem. Int. Ed. 45 (2006) 5492.
[18] Y.-M. Jeon, G. S. Armatas, J. Heo, M. G. Kanatzidis, C. A. Mirkin, Adv. Mater. 20 (2008) 2105.
[19] I. Imaz, D. Maspoch, C. Rodríguez-Blanco, J.-M. Pérez-Falcón, J. Campo, D. Ruiz-Molina, Angew. Chem. Int. Ed. 2008, 47, 1857.
[20] N. Graf, S. J. Lippard, Adv. Drug Deliv. Rev. 64 (2012) 993.
[21] I. Imaz, J. Hernando, D. Ruiz-Molina, D.Maspoch, Angew. Chem. Int. Ed. 48 (2009) 2325.
[22] I. Imaz, M. Rubio-Martínez, L. García-Fernández, F. García, D. Ruiz-Molina, J. Hernando, V. Puntes, D. Maspoch, Chem. Commun. 46 (2010) 4737.
[23] R. P. Batycky, J. Hanes, R. Langer, D. A. Edwards, J. Pharm. Sci. 86 (1997) 1464.
[24] N. Faisant, J. Siepmann, J. P. Benoit, Eur. J. Pharm. Sci. 15 (2002) 355.
[25] J. Wang, B. M. Wang, S. P. Schwendeman, J. Controlled Release, 82 (2002) 289.
[26] C. Berkland, K. Kim, D. W. Pack, Pharm. Res. 20 (2003) 1055.
[27] P. Huang, J. Mao, L. Yang, P. Yu, L. Mao, Chem. Eur. J. 17 (2011) 11390 .
[28] K. Wang, X. Ma, D. Shao, Z. Geng, Z. Zhang, Z. Wang, Cryst. Growth Des. 12 (2012) 3786.

[29] A. Zanella, V. Gandin, M. Porchia, F. Refosco, F. Tisato, F. Sorrentino, G. Scutari, M. P. Rigobello, C. Marzano Invest. New Drugs 29 (2011) 1213.
[30] W. Cho, Y. H. Lee, H. J. Lee, M. Oh Chem. Comm. (2009) 4756.
[31] L. Kelland, Nat. Rev. Cancer 7 (2007) 573.
[32] J. M. Meerum Terwogt, G. Groenewegen, D. Pluim, M. Maliepaard, M. M. Tibben, A. Huisman, W. W. ten Bokkel Huinink, M. Schot, H. Welbank, E. E. Voest, J. H. Beijnen, J. M. Schellens, Cancer Chemother. Pharmacol. 49 (2002) 201.
[33] P. Sood, K. B. Hurmond, J. E. Jacob, L. K. Waller, G. O. Silva, D. R. Stewart, D. P. Nowotnik, Bioconjugate Chem. 17 (2006) 1270.
[34] R. P. Feazell, N. Nakayama-Ratchford, H. Dai, S. J. Lippard, J. Am. Chem. Soc. 129 (2007) 8438.
[35] W. J. Rieter, K. M. Pott, K. M. L. Taylor, W. Lin, J. Am. Chem. Soc. 130 (2008) 11584.
[36] J. Yang, W. Liu, M. Sui, J. Tang, Y. Shen, Biomaterials 32 (2011) 9136.
[37] W. Lu, V. A. L. Roy, C.-M. Che, Chem. Commun. 38 (2006) 3972.
[38] L. Xing, Y. Cao, S. Che, Chem. Commun. 48 (2012) 5995.
[39] R. C. Huxford, K. E. deKrafft, W. S. Boyle, D. Liu, W. Lin, Chem. Sci. 3 (2012) 198.
[40] J. R. Green, Oncologist 9 (2004) 3.
[41] D. Liu, S. A. Kramer, R. C. Huxford-Phillips, S. Wang, J. Della Rocca, W. Lin Chem. Commun. 48 (2012) 2668.
[42] A. Dautry-Varsat, A. Ciechanover, H. Lodish, Proc. Natl. Acad. Sci. 80 (1983) 2258.
[43] L. Xing, H. Zheng, S. Che, Chem. Eur. J. 17 (2011) 7271.
[44] K. M. L. Taylor, J. S. Kim, W. J. Rieter, H. An, W. Lin, W. Lin, J. Am. Chem. Soc. 130 (2008) 2154.
[45] Z. P. Xu, N. D. Kurniawan, P. F. Bartlett, G. Q. Lu, Chem. Eur. J. 13 (2007) 2824.
[46] M. A. Sieber, T. Steger-Hartmann, P. Lengsfeld, H. Pietsch, J Magn. Reson. Imaging. 30 (2009) 1268.
[47] M. R. Prince, H. L. Zhang, J. C. Prowda, M. E. Grossman, D. N. Silvers, Radiographics 29 (2009) 1565.
[48] J. M. Idee, M. Port, A. Dencausse, E. Lancelot, C. Corot Radiol Clin North Am. 47 (2009) 855.
[49] J. Huang, L. Bu, J. Xie, K. Chen, Z. Cheng, X. Li, ACS Nano 4 (2010) 7151.
[50] J. Xie, S. Lee, X. Chen, Adv. Drug Deliv. Rev. 62 (2010) 1064.
[51] J. Xie, K. Chen, J. Huang, S. Lee, J. Wang, J. Gao, Biomaterials 31 (2010) 3016.
[52] T. Kim, E. Momin, J. Choi, K. Yuan, H. Zaidi, J. Kim, J. Am. Chem. Soc. 133 (2011) 2955.
[53] (a) P. Caravan, J. J. Ellison, T. J. McMurry, R. B. Lauffer, Chem. Rev. 99 (1999) 2293.
[54] J. S. Kim, W. J. Rieter,K. M. L. Taylor, H. An, W. Lin, J. Am.Chem. Soc. 129 (2007) 8962.
[55] K. M. L. Taylor, W. J. Rieter, W. Lin, J. Am. Chem. Soc. 130 (2008) 14358.
[56] G. Elizondo, C. J. Fretz, D. D. Stark, S. M. Rocklage, S. C. Quay, D. Worah, Y. – M. Tsang, M. C-M.Chen, J. T. Ferrucci, Radiology 178 (1991) 73.
[57] A. P. Alivisatos, Science 271 (1996) 933.
[58] J. K. Jaiswal, H. Mattoussi, J. M. Mauro, S. M. Simon, Nat. Biotechnol. 21 (2002) 47.
[59] M. A. El-Sayed, Acc. Chem. Res. 37 (2004) 326.
[60] N. L. Rosi, C. A. Mirkin, Chem. Rev. 105 (2005) 1547.

[61] C. Burda, X. B. Chen, R. Narayana, M. A. El-Sayed, Chem. Rev. 105 (2005) 1025.
[62] Z. Kang, Y. Liu, C. H. A. Tsang, D. D. D. Ma, X. Fan, N.-B. Wong, S.-T. Lee, Adv. Mater. 21 (2009) 661.
[63] J. K. Jaiswal, H. Mattoussi, J. M. Mauro, S. M. Simon, Nat. Biotechnol. 2003, 21, 47.
[64] B. Dubertret, P. Skourides, D. J. Norris, V. Noireaux, A. H. Brivanlou, A. Libchaber, Science 298, (2002) 1759.
[65] L. Zhang, X. Qian, L. Liu, Z. Shi, Y. Li, S. Wang, H. Liu, Y. Lia, Chem. Commun. 48 (2012) 6166.
[66] S.-L. Zhong, R. Xu, L.-F. Zhang, W.-G. Qu, G.-Q. Gao, X.-L. Wub, A.-W. Xu, J. Mater. Chem. 21(2011) 16574.
[67] C. Aimé, R. Nishiyabu, R. Gondo, N. Kimizuka, Chem. Eur. J. 16 (2010) 3604.
[68] Z. Zhou, D. Li, H. Yang, Y. Zhub, S. Yang, Dalton Trans. 40 (2011) 11941.
[69] Y. Liu, Z. Tang, Chem. Eur. J. 18 (2012) 1030.
[70] C. Ratanatawanate, A. Chyao, K. J. Balkus Jr., J. Am. Chem. Soc. 133 (2011) 3492.
[71] L. Wu, B. G. Quan, Y. L. Liu, R. Song, Z. Y. Tang, ACS Nano 5 (2011) 2224.
[72] M. Nagarathinam, K. Saravanan, W. L. Leong, P. Balaya, J. J. Vittal, Cryst. Growth Des. 9 (2009) 4461.
[73] S. Xiong, B. Xi, C. Wang, G. Zou, L. Fei, W. Wang, Y. Qian, Chem. Eur. J. 13 (2007) 3076.
[74] C. Li, K. Deng, Z. Y. Tang, L. Jiang, J. Am. Chem. Soc. 132 (2010) 8202.
[75] E. V. Anokhina, Y. B. Go, Y. Lee, T. Vogt, A. J. Jacobson, J. Am. Chem. Soc. 128 (2006) 9957.
[76]Y. G. Zhang, M. K. Saha, I. Bernal, Cryst. Eng. Comm 5 (2003) 34.
[77] K. Nomiya, S. Takahashi, R. Noguchi, S. Nemoto, T. Takayama, M. Oda, Inorg. Chem. 39 (2000) 3301.
[78] S. Ahmad, A. A. Isab, S. Ali, A. R. Al-Arfaj, Polyhedron 25 (2006) 1633.

FIGURE CAPTIONS

Figure 1. (a) In vitro release profile of DOX and SN-38 from DOX/Zn(bix) (dot, red) and SN-38/Zn(bix) (square, green) spheres incubated in pH 7.2 PBS at 37 1C. (b) SEM micrographs of DOX/Zn(bix) spheres taken at 1, 4, 8, and 24 hours, showing representative degradation in pH 7.4 PBS at 37 1C. (c and d) In vitro cytotoxicity assay curves after 24 h for HL60 cells obtained by plotting the cell viability percentage against the (c) Zn(bix) (square, blue) and DOX/Zn(bix) (dot, pink) concentration and (d) the DOX release from DOX/ Zn(bix) spheres (dot, red) and DOX (square, orange) concentration. Reproduced from Ref. [22].

Figure 2. Strategy for the delivery of Pt-based drugs to cancer cells via their inclusion into CPPs stabilized with shells of amorphous silica to prevent rapid dissolution and to effectively control the release of the Pt species. In order to enhance the cellular uptake, a small cyclic peptide silyl-derived c(RGDfK) is finally anchored onto its surface. Reproduced from Ref. [35].

Figure 3. SEM and TEM images of CPNs core (1) and core–shell CPNs (2 and 3): a1: CHG-Fe, a2 and a3: CHG-Fe@BIX-Zn; b1: MTX-Zn, b2 and b3: MTX-Zn@BIX-Zn; c1: MTX-Fe, c2 and c3: MTX-Fe@BIX-Zn; d1: Calcein-Fe, d2 and d3: Calcein-Fe@BIX-Zn. Reproduced from Ref. [38].

Figure 4. Synthesis of CPPs and functionalization of MTX-containing CPPs with a lipid bilayer and targeting moiety. Reproduced from Ref. [39].

Figure 5. Schematic of a pH-responsive system based on coordination bonding in nanoparticles. Route a: At neutral pH 7.0–7.4, ligand molecules with functional groups are coordinated to metal ions and polymerize to form "ligand–metal" nanoparticles. When the external pH of the nanoparticles is reduced, the nanoparticles are disrupted and the ligand molecules detach due to cleavage of the coordination bond. Route b: By introducing host molecules, nanoparticles can be formed with a "host–metal–ligand" architecture. At low pH, the ligand molecules are released from the nanoparticles due to cleavage of either coordination bond. Reproduced from Ref. [43].

Figure 6. (a) Dissolution curves of uncoated (blue) and silica-coated (red) $Mn_3(BTC)_2(H_2O)_6$ nanoparticles in water at 37 °C (% released vs time). (b) In vitro MR images of HT-29 cells incubated with no silica-coated (left), nontargeted silica-coated (middle), and c(RGDfK)-targeted silica-coated (right). (c-e) Merged confocal images of HT-29 cells that were incubated with no 2′ (c), nontargeted silica-coated (d), c(RGDfK)-targeted silica-coated (e). The blue color was from DRAQ5 used to stain the cell nuclei while the green color was from rhodamine B. The bars represent 20 μm. Reproduced from Ref. [56]

Figure 7. (a) TEM image and (b) HRTEM image of PZn QDs, the inset is the corresponding HRTEM image. Reproduced from Ref. [65].

Figure 8. a) A scheme and transmission electron microscopy (TEM) image of the AuIII–adenine colloidal particles obtained by simply mixing the precursor aqueous solutions of adenine and HAuCl4. b) A scheme and scanning electron microscopy (SEM) image of nanoparticles formed by self-assembly of 5'-AMP and Lanthanide ions (Gd3+). Reproduced from reference [69].

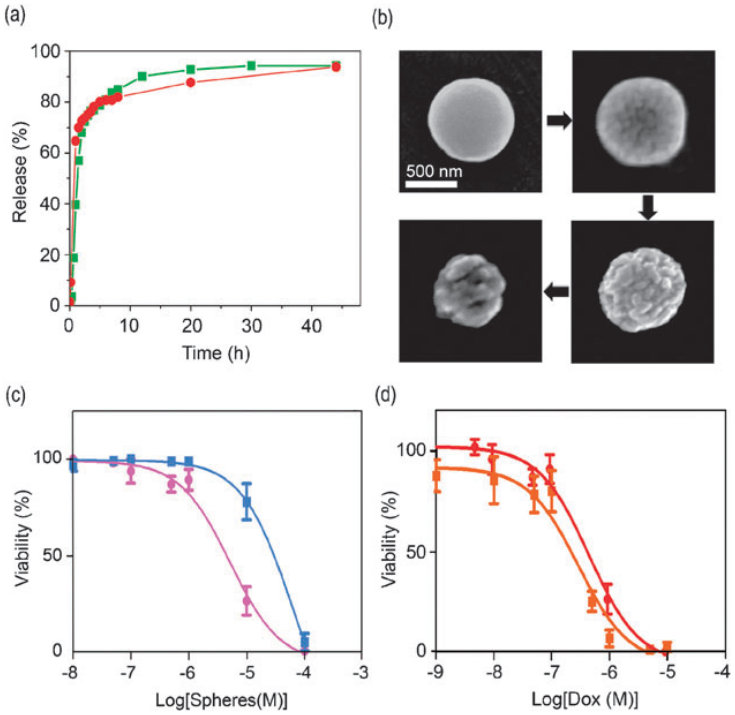
(a)
Release (%)
Time (h)
(b)
500 nm
(c)
Viability (%)
Log[Spheres(M)]
(d)
Viability (%)
Log[Dox (M)]

Figure 1

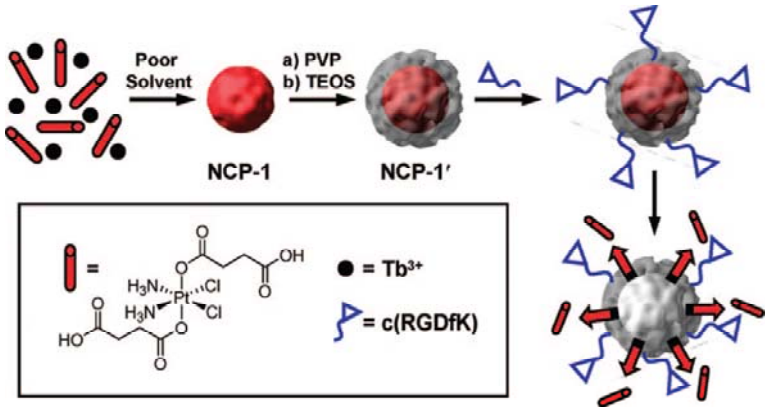

Figure 2

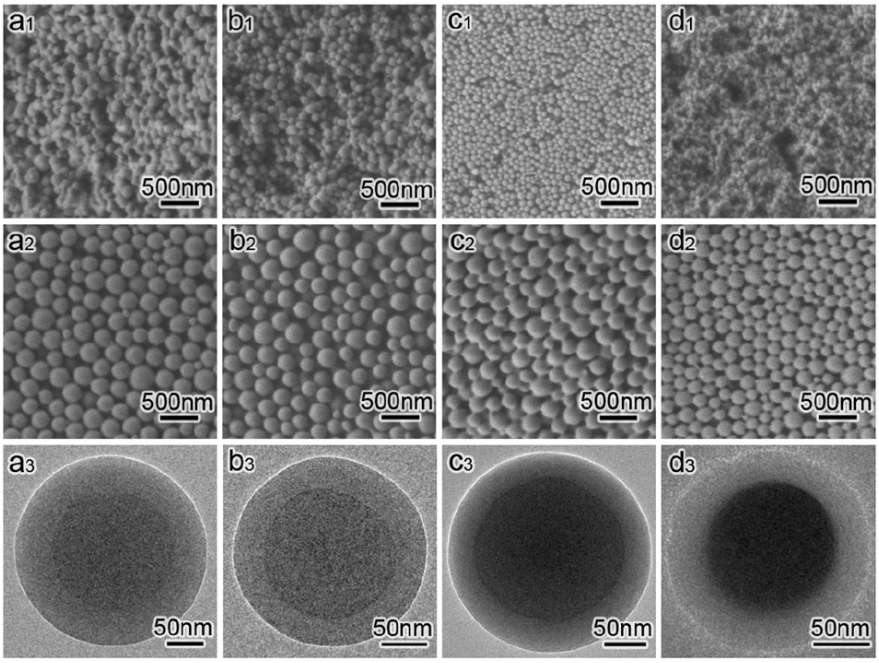
a1
500nm
b1
500nm
c1
500nm
d1
500nm
a2
500nm
b2
500nm
c2
500nm
d2
500nm
a3
50nm
b3
50nm
c3
50nm
d3
50nm

Figure 3

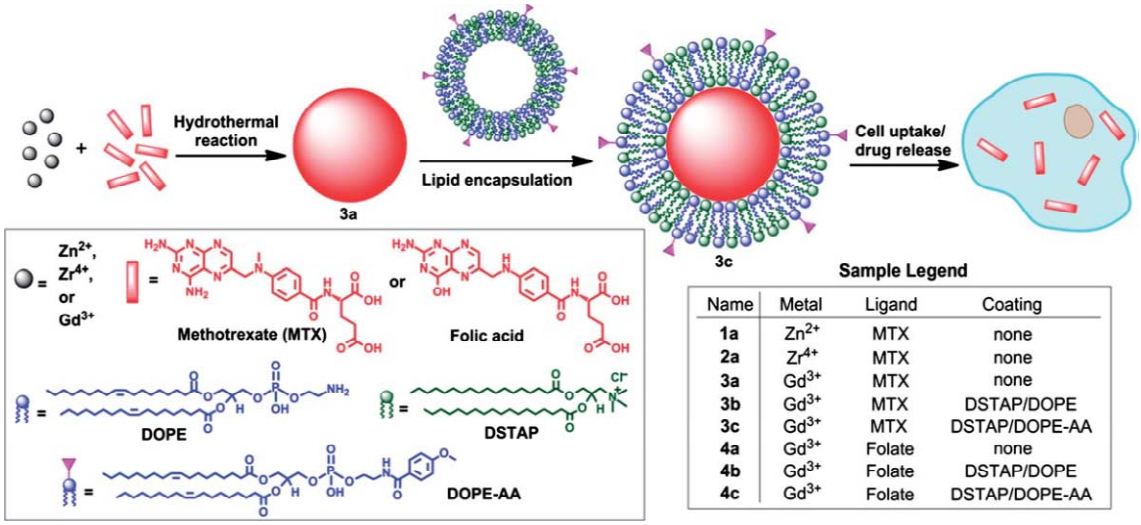

Sample Legend

Name	Metal	Ligand	Coating
1a	Zn^{2+}	MTX	none
2a	Zr^{4+}	MTX	none
3a	Gd^{3+}	MTX	none
3b	Gd^{3+}	MTX	DSTAP/DOPE
3c	Gd^{3+}	MTX	DSTAP/DOPE-AA
4a	Gd^{3+}	Folate	none
4b	Gd^{3+}	Folate	DSTAP/DOPE
4c	Gd^{3+}	Folate	DSTAP/DOPE-AA

Figure 4

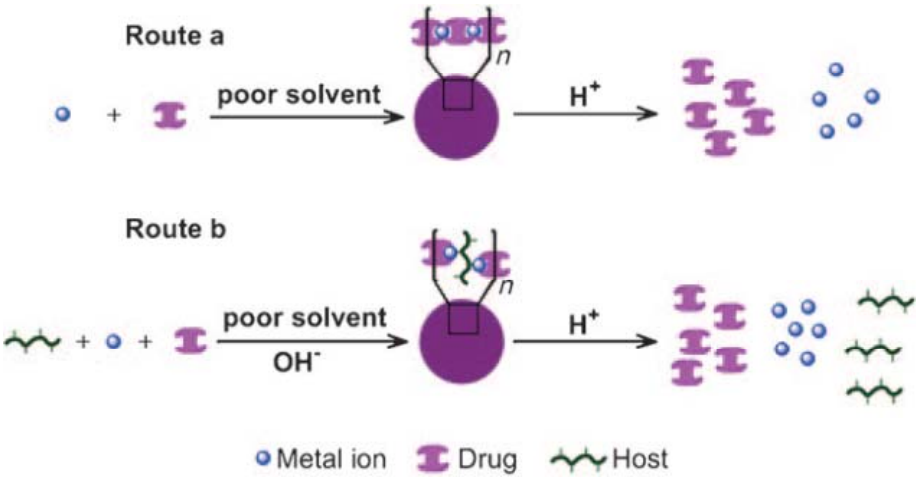
Route a
poor solvent
n
H+
Route b
poor solvent
OH-
n
H+
Metal ion
Drug
Host

Figure 5

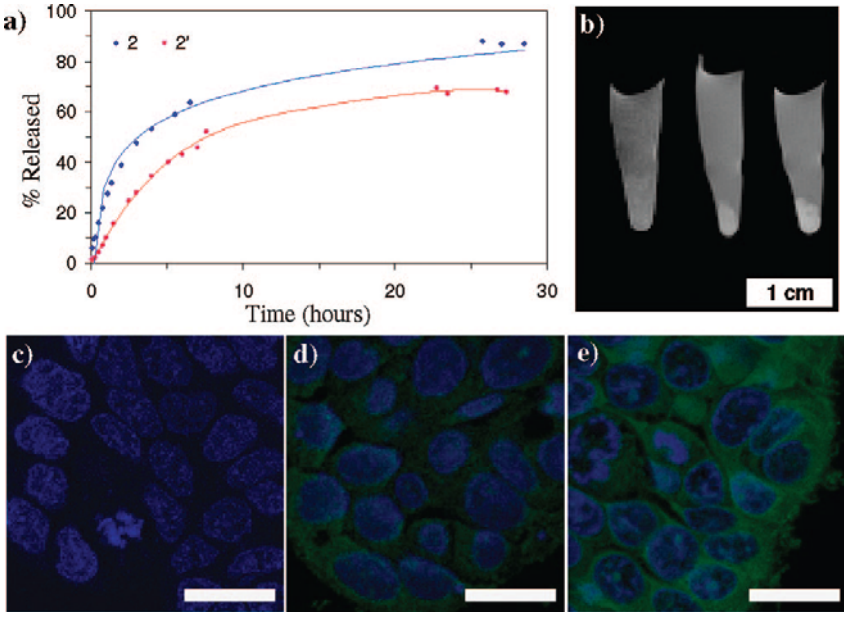

Figure 6

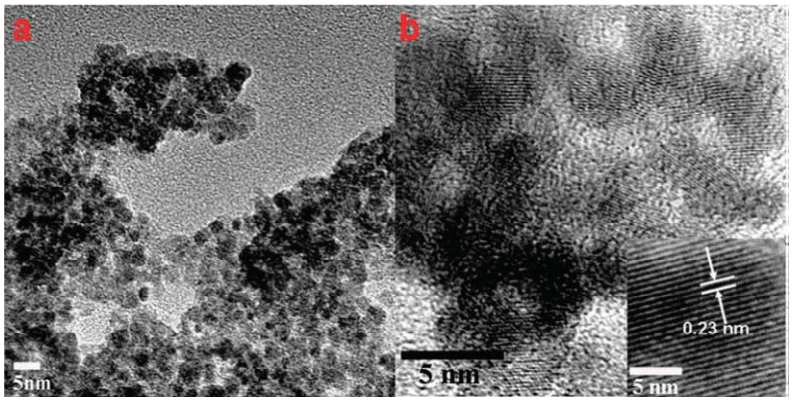

Figure 7

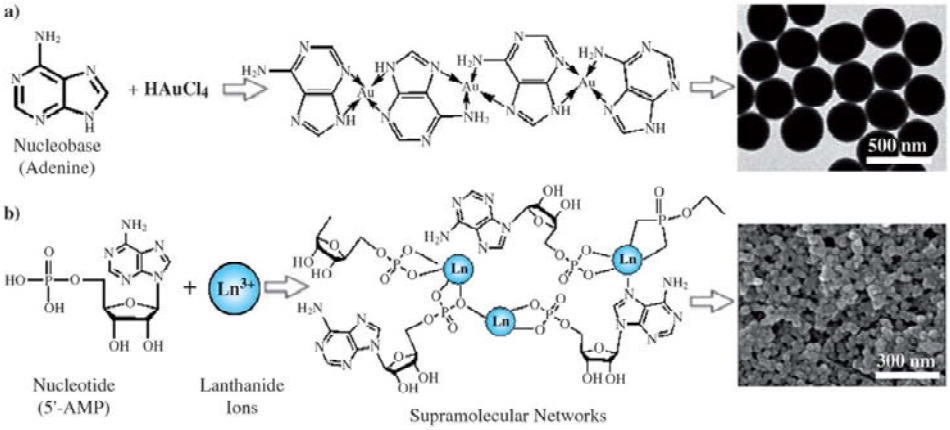
a)
+ HAuCl4
Nucleobase
(Adenine)
500 nm
b)
Nucleotide
(5'-AMP)
Lanthanide
Ions
Supramolecular Networks
300 nm

Figure 8